

Photoresponse above 85 K of selective epitaxy grown high- T_c superconducting microwires

Cite as: Appl. Phys. Lett. **117**, 032602 (2020); <https://doi.org/10.1063/5.0006584>
 Submitted: 04 March 2020 • Accepted: 01 July 2020 • Published Online: 20 July 2020

X. Xing,  K. Balasubramanian,  S. Bouscher, et al.



View Online



Export Citation



CrossMark

ARTICLES YOU MAY BE INTERESTED IN

[Superconducting nanowire single-photon detectors: A perspective on evolution, state-of-the-art, future developments, and applications](#)

Applied Physics Letters **118**, 190502 (2021); <https://doi.org/10.1063/5.0045990>

[Picosecond superconducting single-photon optical detector](#)

Applied Physics Letters **79**, 705 (2001); <https://doi.org/10.1063/1.1388868>

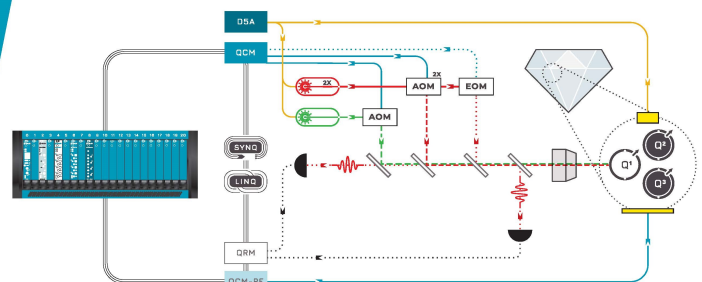
[Progress on large-scale superconducting nanowire single-photon detectors](#)

Applied Physics Letters **118**, 100501 (2021); <https://doi.org/10.1063/5.0044057>

 QBLOX

Integrates all
Instrumentation + Software
for Control and Readout of
NV-Centers

[visit our website >](#)



Photoresponse above 85 K of selective epitaxy grown high- T_c superconducting microwires

Cite as: Appl. Phys. Lett. **117**, 032602 (2020); doi: [10.1063/5.0006584](https://doi.org/10.1063/5.0006584)

Submitted: 4 March 2020 · Accepted: 1 July 2020 ·

Published Online: 20 July 2020



View Online



Export Citation



CrossMark

X. Xing,¹ K. Balasubramanian,¹  S. Bouscher,¹  O. Zohar,¹  Y. Nitzav,² A. Kanigel,² and A. Hayat^{1,a)} 

AFFILIATIONS

¹Department of Electrical Engineering, Israel Institute of Technology, Haifa 3200003, Israel

²Department of Physics, Israel Institute of Technology, Haifa 3200003, Israel

^{a)}Author to whom correspondence should be addressed: alex.hayat@technion.ac.il

ABSTRACT

Superconducting single-photon detectors have become a very promising infrared photon counting technology. Utilizing high- T_c superconductors to implement photon counters is significantly more practical due to their much higher operating temperatures. We report photoresponse above 85 K of $\text{YBa}_2\text{Cu}_3\text{O}_{7-\delta}$ (YBCO) microwires fabricated using selective epitaxial growth (SEG), demonstrating their high photon detection efficiency. SEG does not require post-deposition treatment of the YBCO layer, thus avoiding material damage and degradation, typically occurring in conventional submicrometer YBCO device fabrication. Our results show excellent superconducting performance with a T_c of up to 89 K and a sharp transition width of $\Delta T \sim 2$ K, as well as a relatively high critical current density J_c of $\sim 5.7 \times 10^5$ A/cm² at 77 K. The optical response of our YBCO microwires, especially the high responsivity of $\sim 3 \times 10^3$ mV/(nW/μm²), paves the way for infrared single-photon detection using high- T_c superconductors.

Published under license by AIP Publishing. <https://doi.org/10.1063/5.0006584>

Photon detectors are widely employed in various classical applications involving extremely low light intensities, such as optical communications¹ and biological imaging.² They are also the indispensable driving force of the revolution in experimental quantum optics, related closely to various quantum information applications implemented over the past decade,³ including quantum key distribution,⁴ optical quantum computing,⁵ and quantum emitter characterization.⁶ Among several approaches in developing photon detectors, superconducting nanowire single-photon detectors (SNSPDs) based on conventional superconductors have been well studied in the past decade, bringing these devices to the commercial level.⁷ SNSPDs are based on superconductors, which typically show a much lower energy gap on the order of \sim meV compared to semiconductors, absorbing photons causing local heating and superconductivity breaking. Therefore, SNSPDs have much broader wavelength ranges compared to those of avalanche photodiode detectors (APDs). These devices offer high detection efficiency over a very broad photon energy range, including mid-IR, low dark counts, and excellent timing resolution reaching the pico-second range.⁷ However, conventional superconductor-based devices require an extremely low operation temperature below 10 K, which limits their commercial applicability.

High- T_c superconductors (HTSs) are ideal candidates for such applications. Since their discovery in 1986, HTSs have been the focus

of much attention due to their relatively high transition temperatures.⁸ Operation temperatures for devices based on HTS materials can be high enough for liquid nitrogen cooling (77 K), allowing the use of cheaper, more flexible, and portable cooling systems. Combined with their fast recovery time,⁹ they are ideal candidates for the next generation of SNSPDs.¹⁰ $\text{YBa}_2\text{Cu}_3\text{O}_{7-\delta}$ (YBCO) is considered here for such devices due to its mature growth techniques.^{11,12} However, during device fabrication, superconducting properties of YBCO tend to undergo significant degradation, leading to device failure. This is mostly attributed to oxygen loss caused by edge damage due to the patterning techniques currently in use.^{13,14} By using complex fabrication procedures to reduce YBCO superconductivity degradation, Arpaia *et al.*^{10,15} obtained nanowires with relatively high J_c that exhibited a fast photoresponse at 10 K albeit with low responsivity. Developing YBCO nanowires for photodetection is thus significantly influenced by the high sensitivity of the superconductivity of YBCO structures to most patterning techniques currently in use,¹¹ and a more robust method for efficient YBCO detector fabrication is required.

Here, we utilize the selective epitaxial growth (SEG) method, in which YBCO deposition is performed as the final step of fabrication—in contrast to the commonly used methods. This fabrication method significantly reduces the risk of degradation. In this approach, a mask

layer that prohibits superconducting YBCO growth is deposited on the substrate followed by patterning of this mask to unveil the underlying substrate. YBCO is then deposited on the patterned substrate. Due to the presence of the masking layer, YBCO grows in the gap directly forming the microwire without any patterning-related degradation taking place. Ma *et al.*¹⁶ used a patterned Si masking layer on MgO substrates to achieve submicrometer YBCO structures, while Fork *et al.*¹⁷ implemented selective epitaxy in an inverted fashion, depositing yttria-stabilized zirconia (YSZ) mask on the Si substrate.

For the fabrication of our microwires, SrTiO₃ (STO) substrates were covered with a plasma-assisted chemical vapor deposition of 60 nm thick SiN_x films. The SiN_x films were patterned using electron beam lithography to expose the microwire patterns, as shown in Fig. 1. The patterned regions of SiN_x were etched using reactive ion etching, as shown in Fig. 1(c). The regions, in which the STO substrate was exposed, were tested using energy dispersed spectroscopic techniques in the scanning electron microscope to ensure complete removal of the SiN_x layer. Finally, YBCO was deposited on the patterned films using pulsed laser deposition (PLD) at 900 °C, as shown in Fig. 1(d). The resulting YBCO that grew on the substrate remains crystalline and retains its superconducting properties.^{18,19} This process allows us to obtain microscale features without degrading the YBCO, which is crucial for the fabrication of narrow photodetectors. Finally, a 50 μm-long selective epitaxial (SE) microwire with a 100 nm thickness and a 10 μm width was obtained, exhibiting $J_c \sim 5.7 \times 10^5$ A/cm² at 77 K. The main challenge in the selective epitaxial growth method we present is the width of the wires. Diffusion from the SiN_x insulating layer into the YBCO has a detrimental effect on its quality, and we believe that this is the limiting factor for the wire width. In our current work, we have chosen a thickness of 100 nm, while the surrounding SiN is only 60 nm thick. This ensures that YBCO layers, unaffected by the lateral diffusion from SiN_x, exist.

While the SEG method is capable of producing wires with widths down to several hundreds of nanometers, since this fabrication method is new and was not fully optimized, the sample yield varied greatly. The yield was especially low (<10%) for wires with

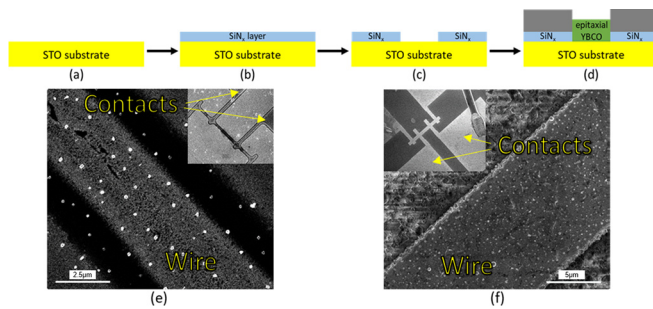


FIG. 1. (a) STO substrate. (b) A layer of SiN_x is deposited on top of the STO substrate. (c) Selected areas of the SiN layer are etched away to reveal the underlying substrate. (d) YBCO is grown over the entire sample, but crystalline YBCO forms only over the areas where the STO substrate was revealed (amorphous layer is marked in gray). Scanning electron microscope (SEM) images of (e) a microwire by PLD and wet etched method and (f) a selective epitaxial microwire. Compared to the microwire in (e), it is distinctly observed that the SE microwire side boundaries form between the crystalline YBCO and the amorphous layer without the etched region, proving the validity of the SEG method.

submicrometer widths, with the samples eventually degrading and losing superconductivity, and while we have fabricated submicrometer wires with widths down to 150 nm, the wires rapidly degraded preventing any meaningful measurement and are thus not discussed in this work. Wires with widths wider than 1 μm had a much higher yield (>80%). We believe that adding proper protection to the wires such as a cap layer could reduce sample degradation over time.

The microwire was put in a closed-cycle optical cryostat system for measurements. A four-probe R(T) measurement was performed to obtain the critical temperature. As shown in Fig. 2(a), a superconducting transition occurred at the onset temperature $T_{onset} \sim 89.6$ K, with an extremely sharp transition ΔT of less than 2 K and a normal resistance of $R_N \sim 550 \Omega$. The sharp change of the resistance at $T = 90.2$ K can be attributed to the electrodes, while the slower change of resistance below this temperature can be attributed to the microwire.

This occurs due to the fact that wide electrodes connected to microwire ends have a slightly different transition temperature than the microwire. Typically, the drop of the electrode resistance occurs about ~1 K above the superconducting transition of the microwire, which is independent of the microwire’s width considered in this manuscript.¹²

We modeled the experimental R(T) curve using the Langer–Ambegaokar–McCumber–Helferlin (LAMH) theory, which is commonly utilized to describe the dominance of thermal activation phase slips (TAPs) on microwire resistance during superconducting transition^{20,21}

$$R_{LAMH}(T) = \frac{h}{4e^2} \frac{\hbar\Omega_a}{k_B T} \exp\left(-\frac{\Delta F}{k_B T}\right), \quad (1)$$

where $\Delta F = \left(\frac{8\sqrt{2}}{3}\right) \left(\frac{B_c^2}{2\mu_0}\right) A\zeta$ is the energy barrier for phase slip nucleation in a volume given by the coherence length ζ times the cross sectional area of wire A . $\Omega_a = \frac{L}{\zeta} \left(\frac{\Delta F}{k_B T}\right)^{1/2} \tau_{GL}^{-1}$, where τ_{GL} is the GL Ginzburg–Landau (GL) relaxation time, k_B is the Boltzmann constant, and L is the microwire length. For T close to T_c the temperature dependence of the coherence length and the critical magnetic field can be described to good approximation as $\zeta(T) = \zeta_0 \left(1 - \frac{T}{T_c}\right)^{-1/2}$ and $B_c(T) = B_c^0 \left(1 - \frac{T}{T_c}\right)$, where $\zeta_0, B_c^0 = h/(2e\sqrt{8\pi}\lambda_0\zeta_0)$, and λ_0 are the values of ζ, B_c , and the London penetration depth λ at 0 K, respectively. The total resistance of the microwire is expressed as a parallel

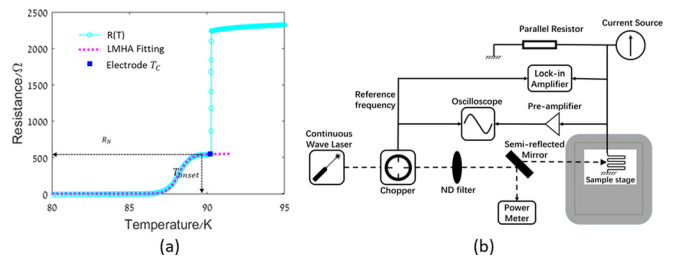


FIG. 2. (a) Resistance vs temperature R(T) measurement (solid line) and Langer–Ambegaokar–McCumber–Helferlin fitting (dotted line) for the SEG microwire. (b) Experimental setup, including the optical path (dashed line) and electrical path (solid line).

combination of R_{LAMH} and normal resistance attributed to quasiparticles,

$$R(T) = (R_{LAMH}^{-1}(T) + R_N^{-1})^{-1}. \quad (2)$$

From the SEG microwire, we extracted $R_N = 550 \Omega$ and fixed the wire length to be $L = 50 \mu\text{m}$ with $T_c = 92 \text{ K}$, $A = 1450 \text{ nm}^2$, $\zeta_0 = 2.58 \text{ nm}$, and $\lambda_0 = 218 \text{ nm}$, which are consistent with the typical values for YBCO.^{22,23} The sharp transition of the SEG microwire demonstrates the advantage of selective epitaxial growth in protecting YBCO microwires from damage and degradation over other methods. Next, we performed photoresponse experiments by illuminating the microwires with an 800-nm CW laser modulated using a chopper at various frequencies around several hundred Hz with the laser intensity controlled by a variable neutral density (ND) filter [Fig. 2(b)]. The laser pulse illuminated the microwire inducing change to its resistance (Figs. 3 and 4). We used an SRS Model SR560 preamplifier with a cut-off frequency of $f_{\text{cutoff}} = 1 \text{ kHz}$ to filter out high-frequency noise. A $3 \text{ k}\Omega$ shunt resistor was placed in parallel to the microwire to protect it from excess current density and to avoid the self-latching effect.^{24,25} The photoresponse for four different bias current densities at 87.5 K and 85.5 K, with a laser intensity of $I_{\text{laser}} = 13.1 \mu\text{W}/\text{mm}^2$ and $3.2 \mu\text{W}/\text{mm}^2$, is shown in Figs. 3 and 4.

Figure 3 clearly reveals the dependence of the photoresponse on temperature, laser intensity, and bias current density. Figures 3(i)–3(iii) show weaker photoresponse at decreased intensity and temperature, respectively. The microwire photoresponse gradually vanished with the decrease in temperature and laser intensity. Bias current density also influences the photoresponse magnitude. At fixed temperature and laser intensity, the photoresponse decreases as the bias current density decreases, for instance, in Fig. 3(i).

To further present the trend of photoresponse dependence on temperature, laser intensity, and bias current density, as shown in Fig. 3, we integrated the photoresponse along the time axis for each

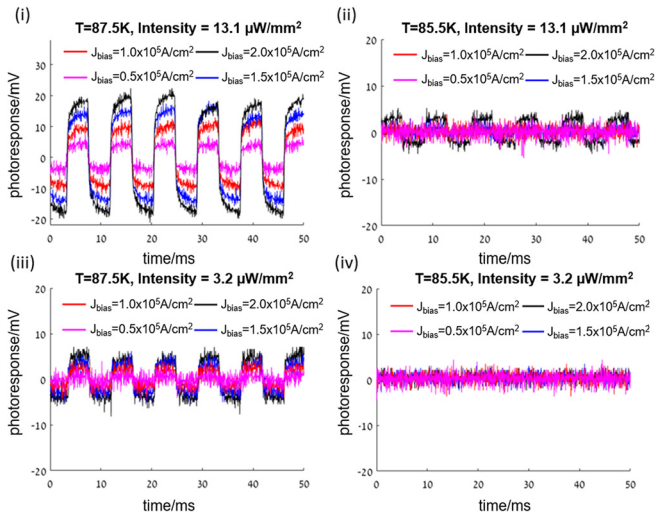


FIG. 3. Photoresponse waveform at different conditions: (i) $T = 87.5 \text{ K}$ and $I_{\text{laser}} = 13.1 \mu\text{W}/\text{mm}^2$, (ii) $T = 85.5 \text{ K}$ and $I_{\text{laser}} = 13.1 \mu\text{W}/\text{mm}^2$, (iii) $T = 87.5 \text{ K}$ and $I_{\text{laser}} = 3.2 \mu\text{W}/\text{mm}^2$, and (iv) $T = 85.5 \text{ K}$ and $I_{\text{laser}} = 3.2 \mu\text{W}/\text{mm}^2$ for different bias current densities.

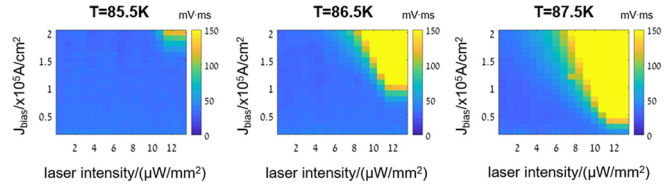


FIG. 4. Integration of the photoresponse waveform at 85.5 K, 86.5 K, and 87.5 K.

given bias current density, laser intensity, and temperature for more measurements (Fig. 4). It demonstrates the positive relation between the bias current density, temperature, laser intensity, and the photoresponse, proving the validity of our analysis mentioned above.

Furthermore, our YBCO microwire demonstrated high responsivity up to several thousand $\text{mV}/(\text{nW}/\mu\text{m}^2)$. A clear dependence of the responsivity on the bias current density and temperature is shown in Fig. 5. As the bias current density approaches the critical value of $J_c \sim 5.7 \times 10^5 \text{ A}/\text{cm}^2$, higher responsivity is observed. For a given bias current density and incident laser intensity, the optimal work temperature is around $T \sim 87.5 \text{ K}$. The responsivity peak in Fig. 5(b) can be attributed to the temperature dependence of the wire's resistance, as shown in Fig. 2(a), as a larger change in the resistance would correspond with a larger voltage change giving higher responsivity. From Fig. 5(a), there is no significant dependence of responsivity on laser intensity. A notable work done previously in the field is the work of Fork *et al.*¹⁷ who fabricated 50 nm-thick and 200 nm-wide YBCO nanowires. A responsivity of $\sim 4 \times 10^{-4} \text{ mV}/(\text{nW}/\mu\text{m}^2)$ was demonstrated at 10 K using a 1.5 μm laser. While our obtained responsivity at 85 K is higher and forms an important milestone, the different dimensions of the wires, as well as the different wavelengths and repetition rates, prohibit a proper comparison.

In conclusion, we demonstrated photoresponse above 85 K of selective epitaxy grown YBCO microwires. The selective epitaxy method can form microwires via the difference between the crystalline YBCO and amorphous regions without any etching involved, which prevents the superconductivity of microwires from degrading. Transport measurements below T_c were performed to obtain the resistance-temperature $R(T)$ dependence, which exhibited bulk-like superconductivity with a T_c of up to 89 K, a sharp superconducting transition, and a J_c of $\sim 5.7 \times 10^5 \text{ A}/\text{cm}^2$ at 77 K. In addition, we observed strong photoresponse, obtaining responsivity as high as $\sim 10^3 \text{ mV}/(\text{nW}/\mu\text{m}^2)$. The microwire photoresponse was shown to

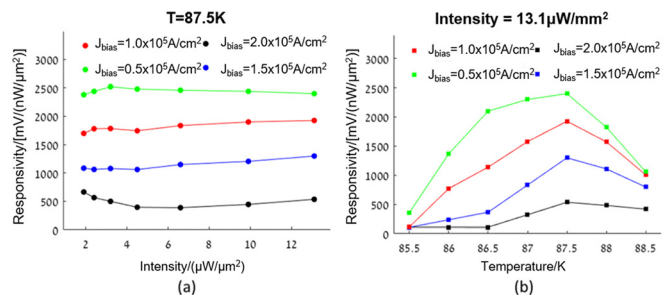


FIG. 5. The dependence of responsivity on (a) incident laser intensity I_{laser} and (b) temperature T .

depend on the bias current density and temperature, as well as laser intensity. Our results demonstrate selective epitaxial growth as a robust fabrication method of efficient photon detectors, which opens a route to single-photon detection based on ultrathin high- T_c superconductors.

AUTHORS' CONTRIBUTIONS

X.X. and K.B. contributed equally to this work.

DATA AVAILABILITY

The data that support the findings of this study are available from the corresponding author upon reasonable request.

REFERENCES

- ¹V. W. S. Chan, "Free-space optical communications," *J. Light. Technol.* **24**, 12 (2006).
- ²E. Grigoriev, A. Akindinov, M. Breitenmoser, S. Buono, E. Charbon, C. Niclass, I. Desforges, and R. Rocca, "Silicon photomultipliers and their biomedical applications," *Nucl. Instrum. Methods Phys. Res., Sect. A* **571**, 130 (2007).
- ³R. H. Hadfield, "Single-photon detectors for optical quantum information applications," *Nat. Photonics* **3**, 696 (2009).
- ⁴C. Gobby, Z. L. Yuan, and A. J. Shields, "Quantum key distribution over 122 km of standard telecom fiber," *Appl. Phys. Lett.* **84**, 3762 (2004).
- ⁵J. Chen, J. B. Altepeter, K. F. Lee, B. Gokden, R. H. Hadfield, S. W. Nam, and P. Kumar, "Demonstration of a quantum controlled-NOT gate in the telecommunications band," *Phys. Rev. Lett.* **100**, 133603 (2008).
- ⁶R. H. Hadfield, M. J. Stevens, S. S. Gruber, A. J. Miller, R. E. Schwall, R. P. Mirin, and S. W. Nam, "Single photon source characterization with a superconducting single photon detector," *Opt. Express* **13**, 10846 (2005).
- ⁷C. M. Natarajan, M. G. Tanner, and R. H. Hadfield, "Superconducting nanowire single-photon detectors: Physics and applications," *Supercond. Sci. Technol.* **25**, 063001 (2012).
- ⁸J. G. Bednorz and K. A. Mueller, "Possible high T_c superconductivity in the Ba-La-Cu-O system," *Z. Phys. B* **64**, 267 (1986).
- ⁹A. D. Semenov, G. N. Gol'tsman, and R. Sobolewski, "Hot-electron effect in superconductors and its applications for radiation sensors," *Supercond. Sci. Technol.* **15**, R1 (2002).
- ¹⁰R. Arpaia, M. Ejrnaes, L. Parlato, F. Tafuri, R. Cristiano, D. Golubev, R. Sobolewski, T. Bauch, F. Lombardi, and G. P. Pepe, "High-temperature superconducting nanowires for photon detection," *Physica C* **509**, 16–21 (2015).
- ¹¹N. Curtz, E. Koller, H. Zbinden, M. Decuroux, L. Antognazza, Ø. Fischer, and N. Gisin, "Patterning of ultrathin YBCO nanowires using a new focused-ion-beam process," *Supercond. Sci. Technol.* **23**, 045015 (2010).
- ¹²S. K. H. Lam and B. Sankrithyan, "HTSC devices fabricated by selective epitaxial growth," *Supercond. Sci. Technol.* **12**, 215 (1999).
- ¹³S. K. H. Lam and S. Gnanarajan, "The investigation of transport properties on $\text{YBa}_2\text{Cu}_3\text{O}_{7-x}$ step edge junctions by ion beam etching," *Physica C* **385**, 466 (2003).
- ¹⁴P. Larsson, B. Nilsson, and Z. G. Ivanov, "Fabrication and transport measurements of $\text{YBa}_2\text{Cu}_3\text{O}_{7-x}$ nanostructures," *J. Vac. Sci. Technol., B* **18**(1), 25–31 (2000).
- ¹⁵R. Arpaia, M. Ejrnaes, R. Cristiano, M. Arzeo, T. Bauch, S. Nawaz, F. Tafuri, G. P. Pepe, and F. Lombardi, "Highly homogeneous YBCO/LSMO nanowires for photoresponse experiments," *Supercond. Sci. Technol.* **27**(4), 044027 (2014).
- ¹⁶Q. Y. Ma, E. S. Yang, G. V. Treyz, and C.-A. Chang, "Novel method of patterning YBaCuO superconducting thin films," *Appl. Phys. Lett.* **55**, 896 (1989).
- ¹⁷D. K. Fork, A. Barrera, T. H. Geballe, A. M. Viano, and D. B. Fenner, "Reaction patterning of $\text{YBa}_2\text{Cu}_3\text{O}_{7-\delta}$ thin films on Si," *Appl. Phys. Lett.* **57**, 2504 (1990).
- ¹⁸C. A. J. Damen, H.-J. H. Smilde, D. H. A. Blank, and H. Rogalla, "Selective epitaxial growth for YBCO thin films," *Supercond. Sci. Technol.* **11**, 437 (1998).
- ¹⁹J. P. Sydow, M. Berninger, R. A. Buhrman, and B. H. Moeckly, "Effects of oxygen content on YBCO Josephson junction structures," *IEEE Trans. Appl. Supercond.* **9**, 2993 (1999).
- ²⁰J. S. Langer and V. Ambegaokar, "Intrinsic resistive transition in narrow superconducting channels," *Phys. Rev.* **164**, 498 (1967).
- ²¹K. Xu and J. R. Heath, "Controlled fabrication and electrical properties of long quasi-one-dimensional superconducting nanowire arrays," *Nano Lett.* **8**(1), 136–141 (2008).
- ²²K. Fossheim and A. Sudbø, *Superconductivity: Physics and Application* (John Wiley & Sons, West Sussex, 2005), p. 173.
- ²³S. Nawaz, T. Bauch, and F. Lombardi, "Transport properties of YBCO nanowires," *IEEE Trans. Appl. Supercond.* **21**, 164 (2011).
- ²⁴J. K. W. Yang, A. J. Kerman, E. A. Dauler, V. Anant, K. M. Rosfjord, and K. K. Berggren, "Modeling the electrical and thermal response of superconducting nanowire single-photon detectors," *IEEE Trans. Appl. Supercond.* **17**, 581 (2007).
- ²⁵D.-K. Liu, S.-J. Chen, L.-X. You, Y.-L. Want, S. Miki, Z. Wang, X.-M. Xie, and M.-H. Jiang, "Nonlatching superconducting nanowire single-photon detection with quasi-constant-voltage bias," *Appl. Phys. Express* **5**, 125202 (2012).